Received: July 1, 2024. Revised: July 22, 2024.

International Journal of
Intelligent Engineering & Systems

http://www.inass.org/

Optimal Power Flow Solution Integrated with TCSC to Improved Voltage Profile and Losses Reduction in Power System Using Effective Intelligent Technique

Inaam Ibrahim Ali[1]* **Shatha Suhbat Abdulla Al-kubragyi[1]**

[1]*Department of Electrical Engineering, Technology University, Baghdad, Iraq*
* Corresponding author's Email: inaam.i.ali@uotechnology.edu.iq

Abstract: One of the most important problems for energy management in power systems is optimal power flow (OPF). Typically, OPF takes into account both the equality and inequality constrictions and optimally modifies the electrical grid's control variables in order to minimize the different objective functions. In this study, a suggested cheetah optimizer-particle swarm optimization (CHO-PSO) approach is implemented for the best possible distribution of TCSC units in electrical power grids, to reduce total system power losses. Furthermore, the OPF problem of the power system with and without the TCSC device is solved using a modified Cheetah optimizer (CHO-PSO) algorithm. The CHO algorithm was recently developed as an effective optimization algorithm based on imitating particular cheetah hunting strategies. Basically, the proposed algorithm introduces the idea of leaving the prey and heading back home to avoid local optimal points. The significant benefit of the CHO method over the other metaheuristic methods is the CHO method's ability to function without the need for algorithm-specific parameters. Two test systems (standard IEEE 30-buses and the Iraqi power grid(IPG) are simulated with and without TCSC device to minimize two objective functions, including transmission active power loss and voltage deviations, while maintaining power balance constraints, voltage and the loading of transmission line limits, in addition to the physical boundaries of TCSC unit. The results are compared with some of the results of other algorithms that have been addressed in the latest literature. For the first system, without TCSC allocation and compared to the HFSS and HGS algorithms, the proposed CHO-PSO achieved a 0.2376 MW and 0.5793 reductions in power losses respectively. Additionally, compared to the HGS, the suggested CHO-PSO algorithm achieves a noteworthy reduction in voltage deviation from 0.1195p.u to 0.1013p.u. Similarly, with TCSC placement, 0.3144 MW less is achieved in power losses by the suggested CHO-PSO in comparison to the SSA. Furthermore, the suggested CHO-PSO is implemented for the best possible distribution of TCSC devices in transmission power systems, to reduce total system losses. Thus, the outcomes show that the suggested algorithm provides an excellent and efficient solution in terms of the power flow problem of electrical systems integrating FACTS units.

Keywords: Optimal power flow, Cheetah optimizer algorithm, Thyristor control series capacitor, Power losses minimization.

1. Introduction

The optimal power flow (OPF) has attracted a lot of researches throughout the last years because of its significance for power system functioning. Optimal power flow has an essential role for effective planning and improving the performance of electric power networks. The main role of optimal power flow finding the optimum or most secure operating point (control variables) for certain objective functions while meeting the limitations on inequality and equality in the system [1]. Control variables include the generation unit's actual power output, the voltage at the power voltage bus, the tap tuning of the transformers, and the reactive sources compensators that are joined to the transmission lines in order to meet the equality and inequality criteria. While the generator's reactive powers, load bus voltages, system voltage stability index, active power losses in transmission lines, and line flows are the problem's dependent variables [2]. The first introduction of the OPF problem formula was in the 1962 [3] and it has

remained a basic optimization problem in the analysis of electrical power systems. There are two tasks of solving OPF. Initially, the computational budget is restricted because it is an operational level problem that is resolved every few minutes. Secondly, for a massive power network with thousands of buses, generators, and loads, it is a non-convex optimization problem. The problem's significance and above described challenges have led to a wealth of literature.

Several traditional optimization techniques, including the Newton method [4], nonlinear programming [5], sequential quadratic programming [6], interior point technique, and linear programming [7] and generalized reduced gradient method have been used to solve the OPF problem. A thorough list of the most widely used conventional optimization algorithms for the OPF problem in power systems is provided in Reference [8]. As has been noted, these methods do not obtain globally optimal solutions and cannot be applied to large power systems. In order to overcome the issues with the traditional approaches, researchers have developed metaheuristic techniques for the OPF problem included genetic algorithm (GA) [2], Salp swarm algorithm [9] and some are algorithms that draw inspiration from nature, such as the hybrid cuckoo search algorithm, the artificial bee colony algorithm [10], particle swarm optimization (PSO) [11], and modified flower pollination [12], Gray wolf optimizer (GWO) [13]. Algorithms that draw inspiration from nature share three characteristics: they mimic natural phenomena, they do not require gradient information, and they implicitly depend on random variables. These approaches can be successfully resolved the "non-convex, non-smooth and non-differentiable optimization problems efficiently and effectively". Nevertheless, during the optimization process, the current algorithm encounters difficulties like stagnation, premature convergence, and local optima trapping, which lead to low-quality and sometimes misleading results for real-world problems.

Building new generating units and transmission networks might be more difficult due to the current concerns about energy consumption, conservation, the environment, and rising costs. Therefore, it is necessary to utilize the current transmission networks more effectively. This can be accomplished by integrating flexible alternating current transmission system (FACTS) and renewable sources such as solar energy devices into the power systems [14, 15].

Recently, flexible AC transmission systems (FACTS) have been widely used to boost long transmission line's capacity for power transfer while enhancing system stability. These devices have the ability to regulate the current, voltage, impedance, and phase angle of the power system grid in order to improve system stability, minimize loss, adjust for power factors, and most significantly, manage the flow of active and reactive power and voltage profiles [16, 17]. Therefore, the traditional OPF issue combined with FACTS devices [18] has created new scopes for managing the real and reactive power flow. To address this kind of power system OPF problem, a variety of optimization algorithms have been used including A GA [18], Symbiotic organisms search (SOS) algorithm [19], Modified lightning attachment procedure optimizer (MLAPO) [20], Adaptive Differential Evolution [21], Improved Dwarf Mongoose Optimizer (IDMO) [22], Hybrid Flying Squirrel Search Algorithm (HFSSA) [23], Krill herd algorithm (KHA) [16] etc. The effectiveness of several metaheuristic methods for both single- and multi-objective optimization using FACT devices is explained. In [24] one of the newest stochastic optimization techniques, the Slime Mould Algorithm (SMA) was developed in response to the behaviour of natural slime Mold's oscillation mode for single and multi-objective functions simultaneously.

Among the FACTs devices, a thyristor-controlled series capacitor (TCSC) is an example of a FACTS device [22]. It is possible to redistribute line power flow, regulate bus voltages and, hence, maximize the use of the existing transmission assets. In [9] a salp swarm algorithm (SSA) was suggested to address the OPF issue in a power system that integrates a thyristor-controlled series capacitor (TCSC). Also, in [22] TCSC devices in transmission power systems are investigated using the Improved Dwarf Mongoose Optimizer (IDMO). However, the above algorithms being proven to be effective, they also have certain limitations. The algorithm may show unstable convergence in the final period, be unable to solve optimal power flow (OPF) with complex functions, and be at risk of dropping into the regional of sub-optimum.

According to a review of the literature, several evolutionary optimization strategies have been used to address the traditional OPF problem in power systems. A review of the literature also reveals that optimization techniques are needed to address the OPF problem of the power network equipped with FACTS devices. Researchers worldwide are constantly looking for better meta-heuristics to solve optimization problems, and researchers focused on engineering optimization tasks are also constantly looking for better meta-heuristic algorithms to achieve the same goal.

The cheetah optimizer (CHO) algorithm was recently developed by Akbari [25] as an effective optimization algorithm for imitating particular

cheetah hunting strategies. Three key tactics are used by this algorithm: hunting for prey, waiting, and attacking. To prevent getting trapped in local optimal points, the algorithm introduces the idea of leaving the prey and heading back home. The significant benefit of the CHO method over the other metaheuristic methods is the CHO method's ability to function without the need for algorithm-specific parameters. The CHO algorithm has demonstrated strong performance in resolving complex issues and has been observed to be extremely effective at solving optimization problems in the engineering field with a very quick rate of convergence and minimal processing time. However, its shortcomings are its lack of in-depth research and its restricted capacity for exploration. So, to utilize its benefits while avoiding its drawbacks, hybridization with another algorithm has become the focus of this research.

In this study, the suggested CHO-PSO is implemented to find the best possible distribution of TCSC devices in transmission power systems. Then, the OPF problem of the power system with and without TCSC device is solved using a modified CHO algorithm (hybridization between the CHO and PSO algorithms).

The summary of this paper's main contributions as below:

- A modified optimization algorithm has been created that combines the PSO exploration property with the CHO hunting strategy.

- Based on the leader's position, the search space is regulated and its step length is modified after the population has been sorted. As a result, both local and global search space are obtained easier by the suggested search approach.

- As far as the authors' knowledge, this is the first time that the CHOPSO is a method inspired by cheetah hunting techniques has been used to address the issue of optimizing the power flow problem by simultaneously obtaining optimal TCSC placement.

Two test systems (standard IEEE 30-buses and the Iraqi power grid) are simulated. The OPF problem with TCSC devices of these test power systems is emulated with two objective functions including transmission active power loss (PLoss) minimization and voltage deviations, while maintaining power balance constraints, voltage limits, transmission line limits, and physical limits of FACTS devices. The obtained results are compared with other metaheuristic algorithms based on computational intelligence that have recently been released in the state-of-the-art literature. The remainder of the paper is structured as follows: Section 2 is presented the modelling of TCSC device. Section 3 is introduced the mathematical mode of the OPF problem with TCSC device. In Section 4, the CHO-PSO algorithm is detailed. In Section 5, the simulation results are shown and discussed. In Section 6, the paper's conclusions are finally drawn.

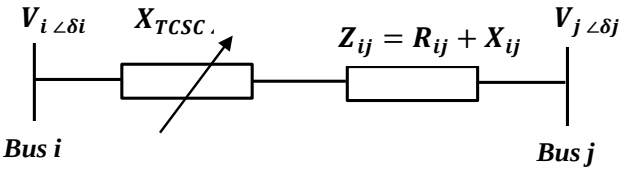

Figure. 1 The TCSC representation coupled to the i-th and j-th buses.

2. Steady-state modelling of TCSC

The modelling of the TCSC device can be represented as a controllable reactance added in series with the relevant transmission line. It is possible to maintain a specific level of real power flow during the compensated transmission line in a variety of operating conditions [9, 19]. In Fig. 1 the network's static model with the TCSC linked between the i-th and j-th buses is displayed. The power flow equations of the line integrated with TCSC are provided by Eqs. (1) and (2) [19].

$$P_{ij} = V_i^2 G_{ij} - V_i V_j G_{ij} \cos(\delta_i - \delta_j) - V_i V_j B_{ij} \sin(\delta_i - \delta_j) \quad (1)$$

$$Q_{ij} = -V_i^2 B_{ij} - V_i V_j G_{ij} \sin(\delta_i - \delta_j) + V_i V_j B_{ij} \cos(\delta_i - \delta_j) \quad (2)$$

Likewise, Eqs. (3) and (4) can be used to express the real and reactive power of the j-th bus.

$$P_{ji} = V_j^2 G_{ij} - V_i V_j G_{ij} \cos(\delta_j - \delta_i) + V_i V_j B_{ij} \sin(\delta_j - \delta_i) \quad (3)$$

$$Q_{ji} = -V_j^2 B_{ij} + V_i V_j G_{ij} \sin(\delta_j - \delta_i) + V_i V_j B_{ij} \cos(\delta_j - \delta_i) \quad (4)$$

where:-

Transmission line conductivity

$$(G_{ij}) = \frac{R_{ij}}{R_{ij}^2 + (X_{ij} - X_{TCSCij})^2}$$

Susceptance of transmission line

$$(B_{ij}) = \frac{X_{ij} - X_{TCSCij}}{R_{ij}^2 + (X_{ij} - X_{TCSCij})^2}$$

P_{ji}, Q_{ji} : Active and reactive power flows, respectively between *i-th* and *j-th* bus.
$V_i V_j$: Voltage magnitudes at i-th and j-th bus respectively.
δ_i, δ_j: Angles at *i-th* and *j-th* bus respectively.
R_{ij}, X_{ij}: Transmission line resistance and reactance between the *i-th* and *j-th* buses.
X_{TCSCij}: The TCSC's reactance in the transmission line that connects the *i-th* and *j-th* buses.

3. Problem formulation with TCSC

OPF solution aims to optimize the power system's steady-state performance with respect to particular objective functions that take equality, inequality and device constraints into account. The OPF problem can be stated mathematically as follows [9, 19]:

$$\text{Minimize} \quad OPF(z_1, z_2) \tag{5}$$

$$\text{Subject to: } \begin{cases} E(z_1, z_2) \\ iE_l \le iE(z_1, z_2) \le iE_u \end{cases} \tag{6}$$

where:
$OPF(z_1, z_2)$: Objective function.
$E(z_1, z_2)$: Numbers of equality limitation.
$iE(z_1, z_2)$: Numbers of inequality limitation.
iE_l, iE_u : set of minimum and maximum of the inequality bounds respectively.
z_1 : Array of dependent variables consisting the active power of slack bus, the reactive powers of generators, load voltages and the loadings on transmission lines.
z_2 : Array of independent variables including of discrete and continuous variables.

The voltage of generators and the active power of the units except the swing bus are represented the continuous variables while the discrete variables are consisted from the tap value settings of transformers, the var compensators and the impedance values of TCSC units. Eqs. (7) and (8) can be used to express z_1 and z_2 respectively.

$$z_1^T = [P_{G1}, Q_{c1 \dots} Q_{cNG}, V_{L1} \dots \dots V_{LNL}, S_{l1} \dots S_{lNTL}] \tag{7}$$

$$z_2^T = [V_{G1} \dots . V_{GNG}, P_{G2} \dots . P_{GNG}, T_1 \dots . T_{NT}, Q_{c1} \dots . Q_{CNC}] \tag{8}$$

where: NG :number of generator buses, NL : sum of loading grid, NTL : sum of transmission lines, NT : sum of controlling transformers and NC : sum of VAR compensators.

- **Objective function**

In this work, to evaluate the effectiveness of the suggested methods, two objective functions are employed separately and simultaneously. The mathematical expressions for the two single objective functions are stated as follows:

i. Minimization of transmission loss.

The objective function to reduce power line losses can be mathematically formulated as follows [19, 20]:

$$F_1(z_1, z_2) = \sum_{R=1}^{NL} G_R [V_i^2 + V_j^2 - 2|V_i|\,|V_j| \cos(\delta_i - \delta_j)] \tag{9}$$

where: G_R represents the conductance of the $K-th$ line between the i-th and j-th buses that connects them.

ii. Voltage Deviation Reduction.

The voltage variation is reduced by using the following expression:

$$min = F_2 = VD = \sum_{i=1}^{Nb} |V_b - 1.0| \tag{10}$$

iii. Constrains

Several equality constraints and inequalities related to dependent and independent variables must be satisfied in order to address the OPF based on the TCSC allocation problem [19].

- **Equality constrains**

The load flow constraints are represented by following equations:

$$\begin{aligned} &\sum_{i=1}^{NB}(P_{Gi} - P_{Li}) + \sum_{i=1}^{NTSCS} P_{is} = \\ &\sum_{i=1}^{NB}\sum_{j=1}^{NB} |V_i||V_j||Y_{ij}|\, cos(\theta_{ij} + \delta_j - \delta_j) \\ &\sum_{i=1}^{NB}(Q_{Gi} - Q_{Li}) + \sum_{i=1}^{NTSCS} Q_{is} = \\ &-\sum_{i=1}^{NB}\sum_{j=1}^{NB} |V_i||V_j||Y_{ij}|\, sin(\theta_{ij} + \delta_j - \delta_j) \end{aligned} \tag{11}$$

Where: P_{Li}, Q_{Li} : are the active and reactive power load of *i-th* bus consequently, P_{Gi}, Q_{Gi} : generator's active and reactive power of *i-th* bus accordingly, P_{is}, Q_{is} : active and reactive powers injection of TSCS unit into the *i-th* bus consequently, Y_{ih} denotes the transmission line admittance between the *i-th* and *j-th* bus, θ_{ij} denotes the admittance angle between the *i-th* and *j-th* bus, NB denotes the number of buses and $NTCCS$ denotes the number of TCCS devices in the power network[22].

- **Inequality constraints**

i. generator restrictions: The *i-th* bus's generator voltage, active power, and reactive power should all

limit between the maximum and minimum values specified by [17]:

$$\begin{aligned} V_{Gi}^{min} < V_{Gi} < V_{Gi}^{Max} \\ P_{Gi}^{min} < P_{Gi} < P_{Gi}^{Max} \\ Q_{Gi}^{min} < Q_{Gi} < Q_{Gi}^{Max} \end{aligned} \quad (12)$$

ii. Eq. (13) control the inequality constrains which included tap settings, reactive power injection from Var sources and TSCS reactance.

$$\begin{cases} T_i^{min} < T_i < T_i^{Max}, \quad i = 1,2,\dots NT \\ Q_{ci}^{min} < Q_{ci} < Q_{ci}^{Max}, \ i = 1,2,\dots NT \\ X_{TCSCi}^{min} < X_{ti} < X_{TCSCi}^{Max} \ \ i = 1,2,\dots NTCSC \end{cases} \quad (13)$$

where:

T_i^{min} and T_i^{Max} :represent the *i-th* transformer's minimum and maximum tap setting limits accordingly.

Q_{ci}^{min} and Q_{ci}^{Max} : the *i-th* shunt capacitor's minimum and maximum VAR injection limits accordingly.

X_{TCSCi}^{min} and X_{TCSCi}^{Max} :are maximum and minimum limits of the of the *i-th TCSC* reactance accordingly and NTCSC: sum of TCSC units located in the power grid.

iii. Additionally, the constraints for load bus and the transmission line loading are addressed by Equation through (14):

$$\begin{aligned} V_{Li}^{min} < V_i < V_{Li}^{Max} \qquad i = 1,2,\dots NL \\ S_{Li} < S_{Li}^{Max} \qquad i = 1,\dots..N_{TL} \end{aligned} \quad (14)$$

Where: V_{Li}^{min} and V_{Li}^{Max} are lower and upper load voltages of *i*-th load bus accordingly, S_{Li}, S_{Li}^{Max} apparent and maximum apparent power flow limit of the *i-th* branch. *N*: The number of transmission lines [19, 22].

4. The proposed algorithm

This section provides an overview of the fundamental concepts of particle swarm optimization (PSO) and cheetah optimization (CHO) techniques. In addition to the proposed hybrid CHO-PSO approach and its flowchart.

Particle swarm algorithm: Particle swarm optimization is a swarm intelligence-based optimization algorithm and metaheuristic global optimization technique. It originates from studies on the movement patterns of fish and birds in flocks. Because it is simple to implement and only requires a small number of tuned particles, the algorithm is widely applied and has been improved quickly. PSO is different from traditional optimization techniques in that it requires only the objective function and does not depend on the gradient or any differential formulas of the problem. Additionally, there aren't many hyper-parameters. The PSO's mathematical formula can be expressed as follows [26]:

$$z_i^{k+1} = z_i^k + v_i^{k+1} \quad (15)$$

$$v_i^{k+1} = w v_i^k + c_1 r_1 (p_i^k - z_i^k) + c_2 r_2 (g_{best} - z_i^k) \quad (16)$$

$$w = w_{max} - ((w_{max} - w_{min}) * (1/Max.iteration)) \quad (17)$$

$\boldsymbol{v_i^k}$: is the velocity vector of particle

$\boldsymbol{z_i^k}$: is particle's vector postion

$\boldsymbol{p_i^k}$: is personal bet postion of particle

$\boldsymbol{g_{best}}$: is the global best position of particle t is the time of initialization

$\boldsymbol{c1}, \boldsymbol{c2}$: are individual and group acceleration coefficients respectively

$\boldsymbol{r1r2}$: are random values of numbers.

$\boldsymbol{W}$: Inertia constant of PSO, w_{max}, w_{min} are the maximum and minimum inertia damping

One of PSO benefits is the ability to move particles around in a multidimensional search area. However, the primary drawback of PSO is that the particle's direction and speed cannot be precisely regulated.

Cheetah Optimizer: The CHO algorithm was first introduced by Akbari et al. [25] and was inspired by cheetah hunting methods. By combined three main steps searching, waiting and attacking, the optimization process can be streamlined in this method. Interestingly, it incorporates a navigation mechanism to escape from a prey position and return to a home location so preventing trapping in suboptimal regions.

i. Searching space: The cheetah keeps a scan on its surroundings and uses its hunting instincts to find the best prey based on the dynamics of the current environment. Mathematically this point can be represented as follows:

$$z_{i,j}^{k+1} = z_{i,j}^k + r \times R_{i,j}^k \quad (18)$$

$$R_{i,j}^{k} = 0.001 \times \frac{k}{k_{max}}(M_{bj} - m_{bj}) \quad (19)$$

where $z_{i,j}^{k}$: represents the current location of cheetah i in arrangement j at iteration k. Every individual cheetah encounters a different kind of prey. Cheetahs exist in various states and represent the population with each individual prey serving as a decision variable that reflects the best possible outcome. Then, the update location of cheetah in each arrangement are renewed according to their previous iteration and a randomly step size, as given in Eqs. (18) and (19), r is expressed as arbitrary number taken between (0, 1) [25, 27].

$R_{i,j}^{k}$ denotes to a random step length and $M_{bj}$and m_{bj} express the maximum and minimum bounds of the variable j in search space. k stands for the current iteration and k_{max} denotes the maximum iteration. The random step distance for additional cheetahs in a group is defined according to the length between cheetah and a randomly chosen cheetah n in a population as below [27]:

$$R_{i,j}^{k} = 0.001 \times \frac{k}{k_{max}}(z_{i,j}^{k} - z_{n,j}^{k}) \quad (20)$$

ii. Sitting-and-Waiting Stage: Cheetahs hunt quickly. It needs a lot of energy to be fast and flexible in the time of the chase. As such, the attack and pursuit last for a short period of time. As a consequence, waiting until the prey is sufficiently close to them is one of the cheetah's key hunting strategies. Then, they launch the attack. This behaviour can increase the success of hunting and is modelled as follows [25, 28]:

$$z_{i,j}^{k+1} = z_{i,j}^{k} \quad (21)$$

iii. Attacking stage: At the right moment, cheetahs need to get as close to their prey as quickly as possible and attack with the highest speed. Here, the prey becomes aware of the cheetah's attack and begins to flee. As a result, the cheetah puts its prey in confusing situations and uses its great degree of flexibility to hunt it. Attacks can happen singly or in groups. The cheetah updates his position in attack mode according to the prey's location. Depending on the prey's and other group member's status, this can be done actively in a simultaneous attack. This point can be formulated mathematically as:

$$z_{i,j}^{k+1} = z_{B,j}^{k} + \check{r}_{i,j} \times \beta_{i,j}^{k} \quad (22)$$

$$\check{r}_{i,j} = \left|\bar{r}_{i,j}\right| \exp\left(\frac{\bar{r}_{i,j}}{2}\right) \sin 2\pi\bar{r}_{i,j} \quad (23)$$

where: the prey position is denoted by $z_{B,j}^{k}$, the turning factor ($\check{r}_{i,j}$) represents the prey's abrupt changes during its flight, and $\bar{r}_{i,j}$ is a random number drawn from a normal distribution. Equation (24) defines the interaction factor as $\beta_{i,j}^{k}$, which can be stated as follows [25]:

$$\beta_{i,j}^{k} = z_{c,j}^{k} - z_{i,j}^{k} \quad (24)$$

where: $z_{c,j}^{k}$denote the positions of cheetahs c at iteration k.

The cheetah should shift its location or go back to its home location if it is unable to capture the prey. If it doesn't find any successful prey in a while, it might move to where the last prey was found and search the area around it. The benefits of cheetah optimization include strength, straightforward and ease of application, adaptive behaviour and quick convergence. Natherless, its shortcomings are its lack of in-depth research and its restricted capacity for exploration. So, to utilize its benefits while avoiding its drawbacks, hybridization with another algorithm has become the focus of recent research.

Hybrid CHO-PSO approach: The main benefit of the merging philosophy of the two algorithms is to combine the exploration potential of the CHO algorithm with the exploitation potential of the PSO algorithm to gain the best features from both variations.

Eqs. (25) to (28) describe the randomization factors. Eq. (28) modifies C_2 which was present in the initial cheetah version. The modification of the current one in the initial PSO optimization to update the leader's follower step is shown in Eq. (30). The following describes the modified mathematical model for determining the leader's position [26]:

$$r_{Hat} = randn \quad (25)$$

$$A = rand\ () \quad (26)$$

$$B = rand\ () \quad (27)$$

$$C_2 = B - \left(\frac{A-B}{Maximumiteration}\right) \quad (28)$$

$$v_i^{k+1} = wv_i^{k} + c_2 r_1 (z_{best}^{k} - z_i^{k}) \quad (29)$$

$$v_i^{k+1} = wv_i^{k} + c_2 r_1 \left(z_b^{k} - z_i^{k}\right) \quad (30)$$

$$z_{i,j}^{k+1} = z_{i,j}^{k} + w \times r_{Hat} \times v_i^{k+1} \qquad (31)$$

where: r_{Hat} , A, B , and C_2 are randomization factors, Z_b^k is the position of the prey, Z_i^k and Z_{best}^k are the current position and the best position of cheetah.

In this paper, the optimal power flow with TCSC unit on the transmission line is solved simultaneously using CHO-PSO approach. The population set of the CHO positions are taken into consideration the best location of TCSC placement as a possible solution during the optimization process beside the state variables of the system with Newton Raphson (NR) algorithm. The algorithm selects the best set of control variables that minimize the target objective function while still meeting the requirements of the system. The recommended procedures for utilizing CHO-PSO approach to solve the OPF problem with compensating TCSC device and NR algorithm are illustrated as flow chart in Fig. 2.

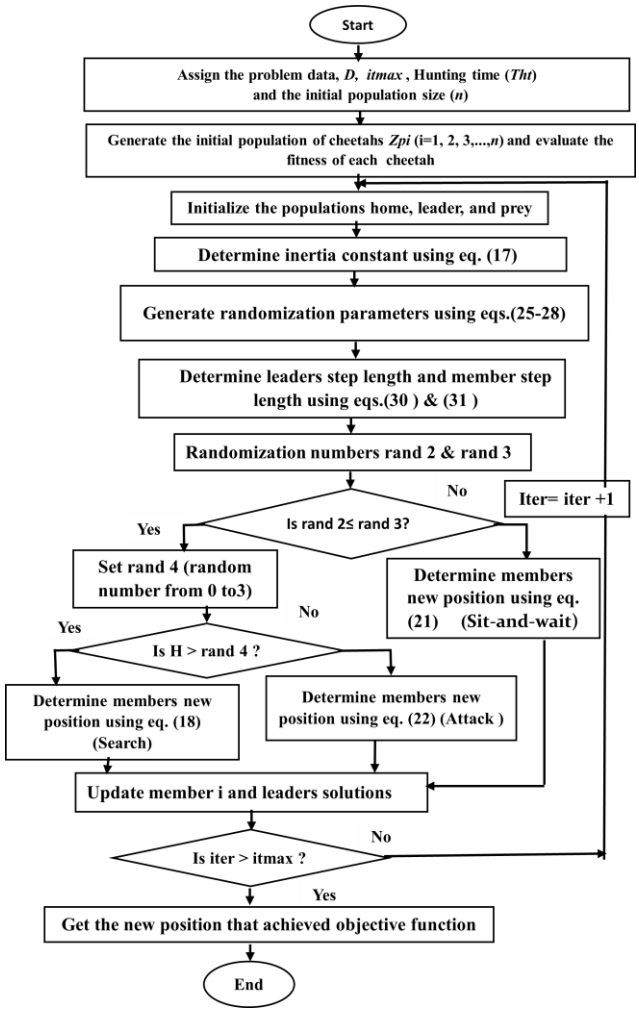

Figure. 2 flowchart of the proposed algorithm CHO-PSO

5. Simulation results

To show the performance of the CHO-PSO method, a 30-bus standard IEEE and the Iraqi power grid (IPG) are simulated in MATLAB program. Using the direct load flow analysis, the control variables, losses, and bus voltage for each system are computed. The final solution of the OPF has been obtained by the suggested optimization algorithm (CHO-PSO). In order to evaluate the efficacy of the suggested algorithm, a comparative analysis is conducted between the overall outcomes and other optimization methods, including the salp swarm algorithm (SSA) [9], Hybrid Flying Squirrel Search Algorithm (HFSS) [23], Improved Dwarf Mongoose Optimizer (IDMO) [22] and Hunger games search (HGS) [1].

The suggested CHO-PSO approach is applied in two scenarios. Firstly, the objective functions simulations are implemented individually and simultaneously in the context of the OPF objective optimization problem without TCSC allocation. Secondly, simulations are applied to solve the OPF problem with TCSC allocation and they are compared to a number of recent metaheuristic algorithms. So, six scenarios have been simulated as below:

- power losses reduction without TCSC placement.
- power losses reduction based on TCSC placement.
- Voltage deviation without TCSC allocation.
- Voltage deviation based on TCSC allocation.
- Minimizing power losses and voltage deviation simultaneously without TCSC allocation.

Minimizing power losses and voltage deviation simultaneously with TCSC allocation.

5.1 30-bus test system

This paper considers a standard 30-bus system as a first test case, as cleared in Fig. 3. The system's data has been depended from [19]. The total demand of the system is 2.834 p.u. at 100 MVA base. The system includes of 6- power units (at buses 1, 2, 5, 8, 11, and 13) and 24 load buses connected by 41 transmission lines of which four lines (6-9, 6-10, 4-12 and 28-27) provide with tap setting transformer and 9 lines are compensating with parallel VAR injection units (at buses 10, 12, 15, 17, 20, 21, 23, 24 and 29). The slack bus is designated as Bus 1. The load bus voltages have been restricted within the range of 0.95 to 1.1 p.u. One TCSC device is placed at Line 22-24 based on the CHO-PSO approach.

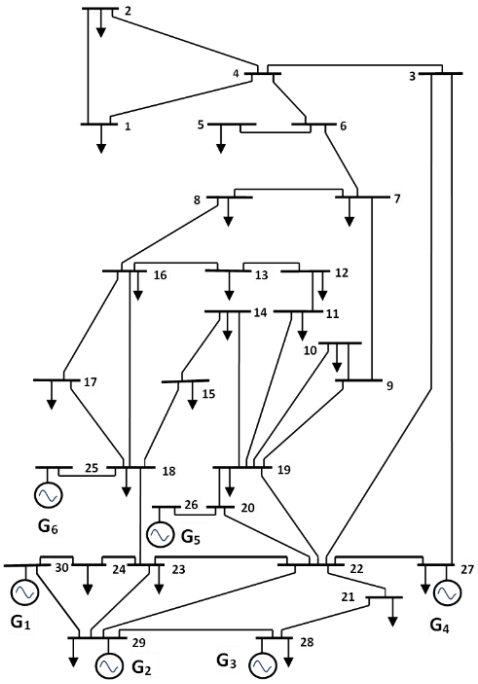

Figure. 3 30-bus system configurations [19]

Two objective functions are employed to validate the suggested algorithm CHO-PSO. In the context of a single objective function of OPF, the functions that are minimized are active power losses [MW] and voltage deviation [p.u], the number of iterations and population size is 200.

 # Case One: In this state, the objective function that the CHO-PSO algorithm minimized is the total power losses [MW] with and without the TCSC device. The overall results of optimal control variables, total power losses and voltage deviation are depicted in Table 1. The findings are contrasted with (SSA) [9] and (HFSS) [23]. The optimal control variables include the output active power of generators except the slack bus, the voltage of the generator buses, tap value setting control of transformers and VAR injection values which are linked with the grid. Without TCSC allocating and

Table 1. The Control Variables Without and with TCSC for the Power Losses optimization (MW) of IEEE -30

Control Variables	Limits		Initial	**without TCSC**			**With TCSC**		
	Min	Max		**Proposed method MCHO-PSO**	**[9] SSA**	**[23] HFSS**	**Proposed method MCHO-PSO**	**[22] IDMO**	**[9] SSA**
P1 [MW]	50	200	99.223	51.3291	51.362	68.6275	52.2959	51.3315	51.340
P2 [MW]	20	80	80	80.0000	80.000	65.2697	79.9068	79.9782	80.000
P3 [MW]	15	50	50	50.0000	50.000	50.000	49.9979	49.9938	50.000
P4 [MW]	10	35	20	35.0000	35.000	28.566	34.9524	34.9473	35.000
P5 [MW]	10	30	20	30.0000	30.000	30.2568	29.9936	29.9884	30.000
P6 [MW]	12	40	20	40.0000	40.000	39.693	39.9534	39.9761	40.000
V1 [p.u.]	0.95	1.1	1.06	1.1000	1.100	1.1	1.1000	1.0997	1.100
V2 [p.u.]	0.95	1.1	1.04	1.1000	1.098	1.0858	1.1000	1.0971	1.097
V3 [p.u.]	0.95	1.1	1.01	1.0867	1.081	1.1	1.0832	1.0784	1.080
V4 [p.u.]	0.95	1.1	1.01	1.1000	1.088	0.9897	1.0922	1.0849	1.087
V5 [p.u.]	0.95	1.1	1.05	1.1000	1.100	0.9658	1.0996	1.0993	1.100
V6 [p.u.]	0.95	1.1	1.05	1.1000	1.038	0.9365	1.1000	1.0999	1.100
T11 [p.u.]	0.9	1.1	1.078	1.1000	1.036	1.0985	1.0996	1.0232	0.979
T12[p.u.]	0.9	1.1	1.069	0.9000	0.918	0.9685	0.9008	0.9376	1.010
T15[p.u.]	0.9	1.1	1.032	1.0026	0.920	0.9796	1.0075	0.9837	0.976
T36[p.u.]	0.9	1.1	1.068	0.9977	0.960	0.9342	1.0015	0.9682	0.954
Qc10[p.u.]	0	5	0	0.0000	30.00	20.5299	5.0000	4.4532	16.899
Qc12[p.u.]	0	5	0	5.0000	NA	NA	4.9998	4.7600	NA
Qc15[p.u.]	0	5	0	5.0000	NA	NA	4.7425	4.0955	NA
Qc17[p.u.]	0	5	0	4.9991	NA	NA	0.0002	4.9950	NA
Qc20[p.u.]	0	5	0	5.0000	NA	NA	4.9984	4.4611	NA
Qc21[p.u.]	0	5	0	5.0000	NA	NA	4.9827	4.9737	NA
Qc23[p.u.]	0	5	0	0.0000	NA	NA	4.9999	2.6629	NA
Qc24[p.u.]	0	5	0	5.0000	11.729	24.0383	4.1019	4.9416	11.412
Qc29[p.u.]	0	5	0	5.0000	NA	NA	4.9995	2.5606	NA
Xtcsc [p.u.]			--------	----------	--------	--------	-0. 19 (at Line 22-24)	-0.4927 (at line 28-27)	0.030 (at line 3-4)
Power loss [MW]			5.6891	2.9311	2.962	3.1687	2.6016	2.8156	2.916
VD [p.u.]			1.1747	1.8729	1.933	-----	1.8100		1.902

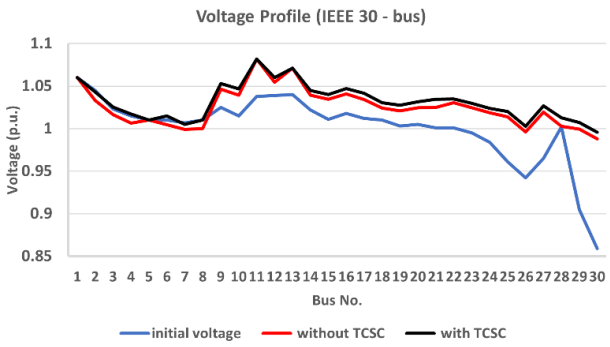

Figure. 4 Voltage profiles of buses without and with TCSC of IEEE 30 -Bus using modified CHO-PSO algorithm (for Case one)

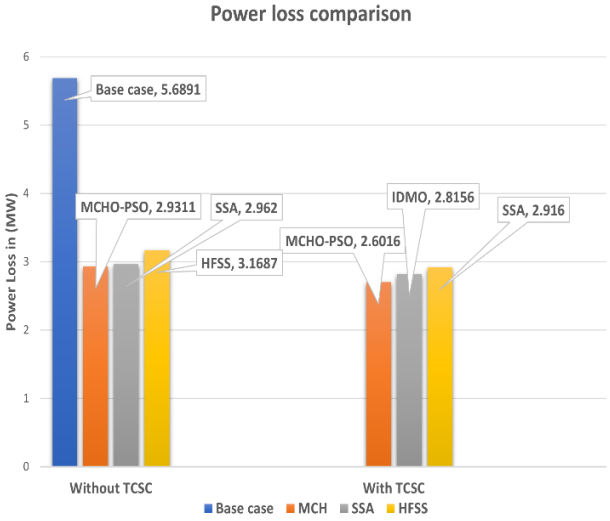

Figure. 5 Power loss comparison of IEEE 30 bus test system

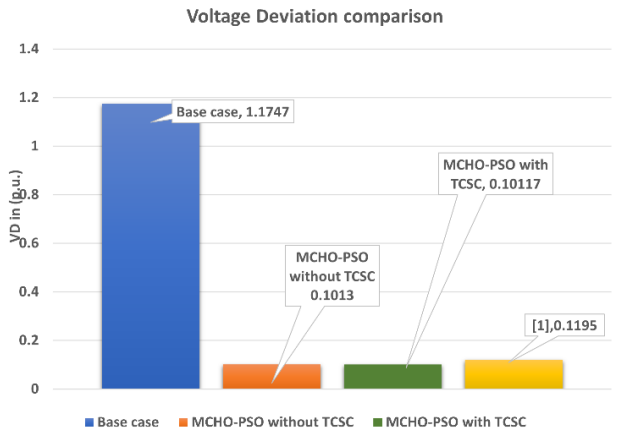

Figure. 6 Voltage Deviation comparison of IEEE 30 bus test system

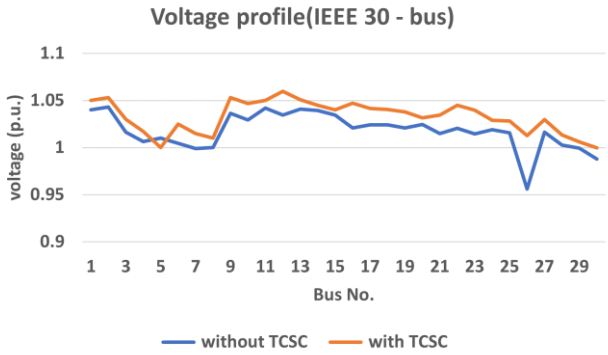

Figure. 7 Voltage profiles of buses without and with TCSC of IEEE 30 -Bus using modified CHO-PSO algorithm. (for Case two)

compared to the original case, the proposed CHO-PSO achieved a 2.758 MW reduction in power losses. When comparing the suggested algorithm's outcomes with the (SSA) also, it achieves a noteworthy reduction in power losses of 0.0309 MW. Additionally, compared to the (HFSS), the suggested CHO-PSO algorithm reduces power losses by 0.2376 MW. Similarly, with TSCS placement at Line (22-24), 3.0875 MW less is achieved by the suggested CHO-PSO in comparison to the original case. In addition, the suggested CHO-PSO obtains a reduction of 0.214 MW and 0.3144 MW in comparison to the results achieves by the (IDMO) [22] and (SSA) [9] respectively.

A comparison of the voltage profiles of buses without and with the TCSC of IEEE 30 buses using a modified CHO-PSO algorithm is plotted in Fig. 4. As it is clear, the voltage magnitude for the base case is less than the minimum limit (0.95 p. u) for some buses. Hence, it has been enhanced with the TCSC device allocated case within the lower and upper limit (0.95 - 1.1) p.u. Also, to illustrate a statistical evaluation of the compared results, Fig. 5 displays the bar plot of power losses according to the outcomes of the compared techniques for case one.

 # Case Two: In this case, the objective function that the CHO-PSO algorithm minimized is the voltage deviation with and without the TCSC device allocated. Table 2 indicates that the proposed CHO-PSO achieved a sum of voltage deviation decreased from 1.1747 p. u to 0.1013 p. u (reduction rate: 90.696%) compared with the base case. When comparing the suggested algorithm's outcomes with the (HGS) [1], it achieves a noteworthy reduction in voltage deviation from 0.1195 p. u to 0.1013 p.u.

Also, the suggested CHO-PSO is used to locate the optimal place of the TCSC device to obtain the lowest possible voltage deviation. Table 2 presents the final control variables for the HGS [1] method and the proposed algorithm CHO-PSO with the corresponding algorithm comparisons shown in Fig. 6. As can be seen, the modified CHO-PSO algorithm

Table 2. The Control Variables Without and with TCSC for the Voltage Deviation Reduction

Control Variables	Limit		Initial	Without TCSC		With TCSC
	Min	Max		Proposed CHO-PSO	[1] HGS	Proposed CHO-PSO
P1 [MW]	50	200	99.223	199.8770	99.3206	131.8377
P2 [MW]	20	80	80	48.5321	56.2324	60.7104
P3 [MW]	15	50	50	48.7621	48.5423	40.4581
P4 [MW]	10	35	20	30.1251	34.7508	18.1646
P5 [MW]	10	30	20	21.7421	19.9674	18.4706
P6 [MW]	12	40	20	19.2117	29.7117	19.2827
V1 [p.u.]	0.95	1.1	1.06	1.02	1.00733	1.0516
V2 [p.u.]	0.95	1.1	1.04	0.9905	0.99464	1.0233
V3 [p.u.]	0.95	1.1	1.01	1.060	1.06787	1.0058
V4 [p.u.]	0.95	1.1	1.01	1.046	1.05785	1.0091
V5 [p.u.]	0.95	1.1	1.05	1.093	1.05771	1.0087
V6 [p.u.]	0.95	1.1	1.05	1.06	0.99197	1.0403
T11 [p.u.]0	0.9	1.1	1.078	1.019	0.97665	0.9274
T12[p.u.]	0.9	1.1	1.069	1.051	0.98726	1.0001
T15[p.u.]	0.9	1.1	1.032	0.9616	0.99930	1.0095
T36[p.u.]	0.9	1.1	1.068	0.98	0.96666	0.9649
Qc10[p.u.]	0	5	0	4.998	3.89253	1.3177
Qc12[p.u.]	0	5	0	0.0355	1.68208	0.5067
Qc15[p.u.]	0	5	0	1.1817	2.33112	3.9135
Qc17[p.u.]	0	5	0	0.7387	3.14785	2.1472
Qc20[p.u.]	0	5	0	4.9755	4.99605	3.9224
Qc21[p.u.]	0	5	0	4.9941	4.06093	3.5943
Qc23[p.u.]	0	5	0	4.9601	4.97509	2.2536
Qc24[p.u.]	0	5	0	4.9662	4.99004	0.9971
Qc29[p.u.]	0	5	0	3.4012	2.55515	3.7415
Xtcsc [p.u.]				----------	----------	-0.19 at Line 22-24
Power loss [MW]			5.6891	5.2501	5.1253	5.9241
VD[p.u.]			1.1747	0.1013	**0.1195**	0.10117

produces the least amount of voltage deviation with TCSC allocation (0.10117 p. u) compared to the other cases. Fig. 7 shows a comparison of bus voltage profiles without and with TCSC for IEEE 30 buses using the modified CHO-PSO algorithm.

 # Case three: Active power losses and voltage deviation are the objective functions that are simultaneously minimized for this example. Table 3 displays the results of the OPF solutions based on CHO-PSO approach for the combined power losses and voltage deviation minimization objective. Without TCSC allocating and compared to the original case, the proposed CHO-PSO achieved a 2.405 MW and 0.5933 p. u reduction in power losses and voltage deviation respectively. Additionally, the results are contrasted with those obtained from other optimization techniques, such as HGS [1]. The table shows that, when compared to the HGS counterpart reported in [1], the proposed CHO-PSO -based algorithm results a sum of losses decreased from 3.8636 MW to 3.2843 MW while the voltage deviation a little increase from 0.2048 p. u to 0.5814 p.u. From other hand, with TCSC considering, the

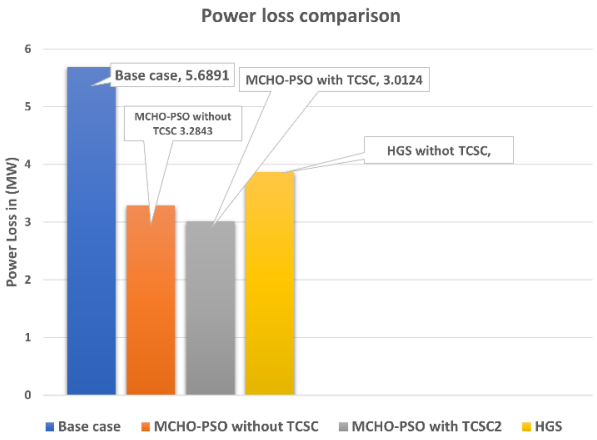

Figure. 8 Power loss comparison of IEEE 30 bus test system.

Table 3. The Control Variables Without and with TCSC for the Power Losses (MW) and voltage deviation reduction of IEEE30- Bus Test System

Control Variables	Limit		Initial	Without TCSC		With TCSC
	Min	Min		Proposed CHO-PSO	[1] HGS	Proposed CHO-PSO
P1 [MW]	50	50	99.223	59.621	62.266	58.987
P2 [MW]	20	20	80	76.710	75.233	77.995
P3 [MW]	15	15	50	50.1021	48.636	48.652
P4 [MW]	10	10	20	33.452	32.980	34.012
P5 [MW]	10	10	20	29.131	29.414	29.298
P6 [MW]	12	12	20	26.9963	38.735	37.0684
V1 [p.u.]	0.95	0.95	1.06	1.051	1.031	1.061
V2 [p.u.]	0.95	0.95	1.04	1.053	1.060	1.042
V3 [p.u.]	0.95	0.95	1.01	1.021	1.002	1.017
V4 [p.u.]	0.95	0.95	1.01	1.048	1.054	1.049
V5 [p.u.]	0.95	0.95	1.05	1.095	1.040	1.095
V6 [p.u.]	0.95	0.95	1.05	1.096	1.010	1.095
T11 [p.u.]	0.9	0.9	1.078	0.962	0.961	0.960
T12[p.u.]	0.9	0.9	1.069	1.008	0.963	1.005
T15[p.u.]	0.9	0.9	1.032	0.952	0.984	0.954
T36[p.u.]	0.9	0.9	1.068	0.002	0.951	0.001
Qc10[p.u.]	0	0	0	0.0001	0.075	0.0
Qc12[p.u.]	0	0	0	0.005	0.000	0.006
Qc15[p.u.]	0	0	0	0.0	0.240	0.001
Qc17[p.u.]	0	0	0	0.0	0.188	0.0
Qc20[p.u.]	0	0	0	0.001	0.782	0.0
Qc21[p.u.]	0	0	0	0.008	4.688	0.007
Qc23[p.u.]	0	0	0	1.03	4.964	1.031
Qc24[p.u.]	0	0	0	0.0	1.196	0.001
Qc29[p.u.]	0	0	0	1.023	0.893	1.022
Xtcsc [p.u.]				----------	----------	-0.19 at Line 22-24
Power loss [MW]			5.6891	3.2843	**3.8636**	3.0124
VD[p.u.]			1.1747	0.5814	**0.2048**	0.3306

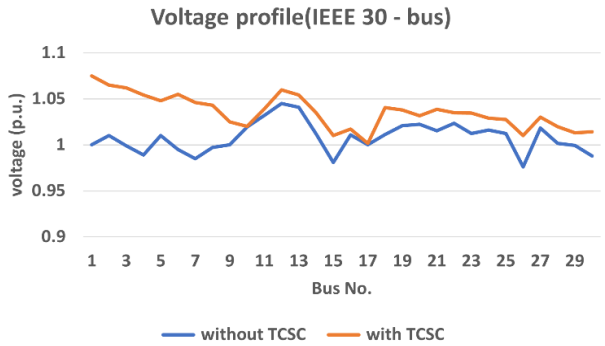

Figure. 9 Voltage profiles of buses without and with TCSC of IEEE 30 -Bus using modified CHO-PSO algorithm. (for Case three)

CHO-PSO achieves 3.0124 MW and 0.3306 p. u in power losses and voltage deviation respectively in comparison to the original case (5.6891 MW and 1.1747p.u) and to the results achieves by the HGS [1] which was (3.8636 MW and 0.2048 p. u). Comparative power losses obvious in Fig. 8 give an effective reduction result in power losses for CHO-PSO approach considering TCSC device. Fig. 9 shows a comparison of bus voltage profiles without and with TCSC for IEEE 30 buses using the modified CHO-PSO algorithm.

5.2 Iraqi test system

The second system tested in this work is the Iraqi Power Grid (IPG). The single line diagram of the system is illustrated in Fig.10. The IPG has twenty-eight buses, twenty-one loads, forty-four lines and twenty-seven control variables. The slack bus is identified by bus number 10 (MUSP) and the total loadings on the system is 5994 MW. System data was adopted from [29].

Table 4. Output of Control Variables Without and with TCSC For Minimizing the Power Losses (MW) and voltage deviation Using IPG 400kV

Control variables	limit		Initial	Single objective function Loss reduction		Multi objective function (loss reduction + voltage deviation)	
	Min.	Max.		Without TCSC	With- TCSC	Without TCSC	With- TCSC
P1	150	1200	159.383	750.420	810..300240	870.432	890.189
P2	130	988	690	972.358	423.751	402.742	352.747
P3	250	750	250	530.870	395.365	442.982	283.441
P4	120	1320	409	541.840	394.800	555.712	315.457
P5	120	636	591	122.010	125.912	325.848	525.243
P6	50	260	240	134.520	104.250	71.645	70.101
P7	180	910	735	201.420	860.420	879.207	880.014
P8	60	660	203	138.155	420.630	280.745	165.341
P9	50	500	369	452.980	175.134	210.393	160.865
P10	250	1320	478	255.721	530.480	520.642	501.541
P11	250	1250	600	542.310	290.055	419.731	408.544
P12	210	840	775	790.200	806.300	705.939	813.921
P13	100	440	332	400.980	435.134	225.914	430.354
P14	50	250	208	190.760	248.753	113.689	215.818
V1	0.95	1.1	1.04	1.03	1.058	1.032	1.041
V2	0.95	1.1	1.02	1.06	1.061	1.034	1.040
V3	0.95	1.1	1.01	1.027	1.059	1.03	1.040
V4	0.95	1.1	1.02	1.02	1.060	1.035	1.041
V5	0.95	1.1	1.02	1.013	1.060	1.05	1.03
V6	0.95	1.1	1.02	1.04	1.053	1.04	1.041
V7	0.95	1.1	1.01	1.021	1.055	1.05	1.04
V8	0.95	1.1	1.02	1.08	1.061	1.035	1.041
V9	0.95	1.1	1.02	1.003	1.057	1.045	1.05
V10	0.95	1.1	1.03	1.035	1.064	1.038	1.041
V11	0.95	1.1	1.03	1.01	1.058	1.045	1.05
V12	0.95	1.1	1.02	0985	1.067	1.035	1.051
V13	0.95	1.1	1.01	1.015	1.044	1.023	1.0040
V14	0.95	1.1	1.01	0.99	1.049	1.03	1.041
Xtcsc [p.u.]			----------	----------	at Line 25-26	----------	at Line 25-26
Power loss [MW]			42.3834	30.5404	27.224	25.621	19.576
VD [p.u.]			0.2013	0.244	0.213	0.235	0.201

The optimal control variables obtained by the suggested approach CHO-PSO are listed in Table 4. For this scenario, the first objective function that the CHO-PSO algorithm minimized is the total power losses with and without the TCSC device. The final control variables and the outputs results produced by the CHO-PSO technique are shown in Table 4.

According to these findings, the active power losses are reduced to 30.5404 MW and 27.224 MW without TCSC and with TCSC allocation respectively compared the base case which is equal to 42.3834 MW. Similarity, the voltage deviation is enhanced to 0.213 p.u in context of considering the TCSC unit as seen in the Table 4. The second function that the CHO-PSO algorithm optimized is a multi-objective including total power losses and voltage deviation with and without the TCSC device. Also, compared to the original case, the suggested CHO-PSO approach reduces power losses to 25.621 MW and voltage deviation to 0.235 p.u. Similarly, with TCSC placement at Line (25-26), the proposed method decreases the power loses to 19.576 MW and the voltage deviation to 0.201 p. u in comparison to the original case.

A comparison of the voltage profiles of buses without and with the TCSC of IPG buses using a modified CHO-PSO algorithm is plotted in Fig. 11.

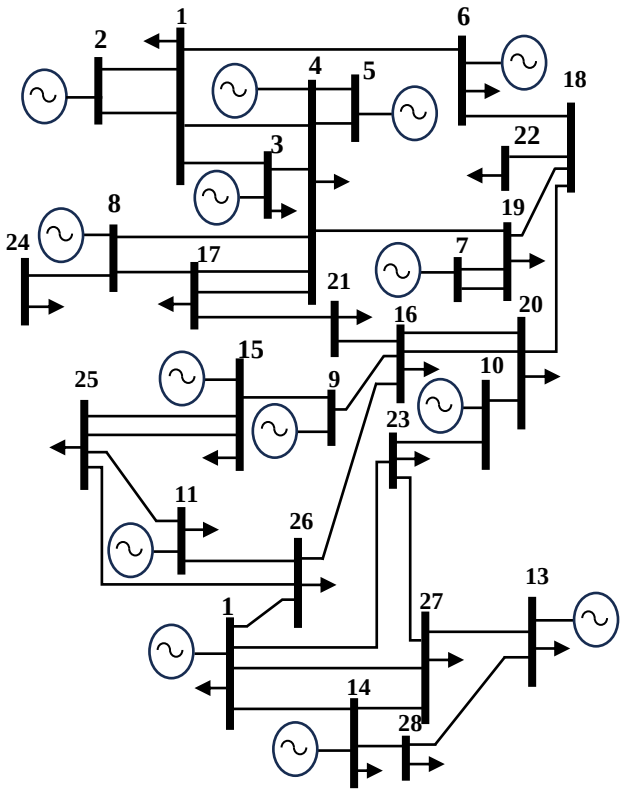

Figure. 10 IPG 400kV configuration [29]

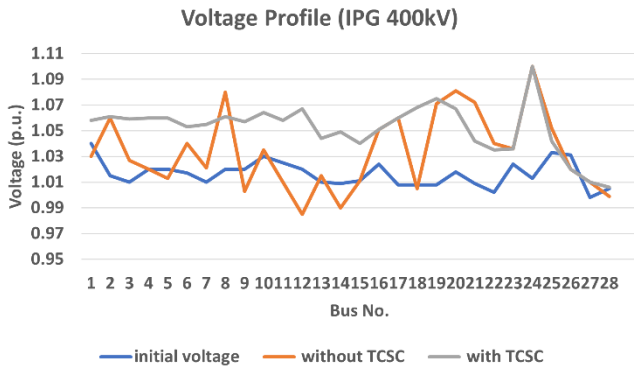

Fig. 11 Voltage Profiles of buses without and with TCSC on IPG 400kV

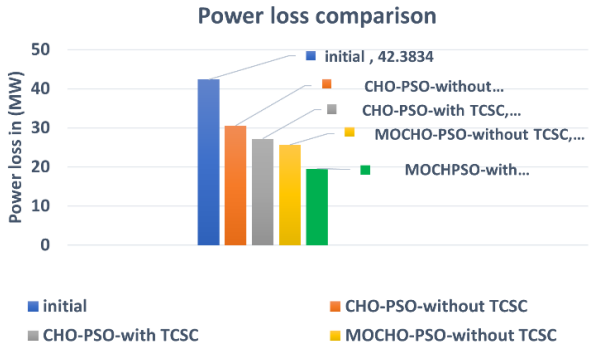

Figure. 12 Power loss comparison of ISG 400kV

Also, to illustrate a statistical evaluation of the compared results, Fig. 12 displays the bar plot of power losses compared to the base case.

6. Conclusion

The OPF problem considering equality and inequality constraints has been solved by using a modified CHO algorithm. It is demonstrated that, the proposed method efficiently optimized the transmission line loss and voltage deviations while maintaining a balance between exploration and exploitation in comparison to the other algorithms. The study takes into account the objectives of voltage deviation minimization and transmission loss minimization separately and simultaneously. The viability of the suggested CHO-PSO method for solving OPF problems is determined using two test systems (standard 30-buses and the Iraqi power grid). After the CHO-PSO approach is validated, TCSC is added to the test grids. It is noted that the functions of losses and voltage deviation under consideration of TCSC unit are further reduced. The obtained results for the OPF problem using CHO-PSO show a promising performance in terms of minimizing power losses and voltage deviation. For the first case system, it's achieving a reduction in losses from 3.2843MW to 3.0124MW without TCSC and with TCSC allocation respectively. Also, the voltage deviation is enhanced from 05814p.u to 0.3306p.u respectively, satisfying all constraints within their respective limits. For the second test system, according to the results, the active power losses are reduced from 25.621MW to 19.576MW without TCSC and with TCSC allocation respectively compared the base case which is equal to 42.3834 MW. Similarity, the voltage deviation is enhanced to 0.235 p. u and 0.201p.u in context of considering the TSCS unit, which indicating the OPF problem will be better solved by implementing CHO-PSO along with TCSC. Thus, it may be suggested that future researchers use the modified CHO algorithm as a very promising algorithm to solve some more challenging engineering optimization problems.

Conflicts of Interest

The authors declare no conflict of interest.

Author Contributions

The first and second authors carried out the background work for the paper, collected the data set, edited the manuscript, analyzed, Software and compared the results.

Notation	Description
c1, c2	Individual and group acceleration coefficients respectively.
g_{best}	Global best position of particle t is the time of initialization.
G_R	The conductance of the $K-th$ line between the i-th and j-th buses.
NB	The number of buses.
$NTCCS$	The number of TCSC devices.
P_{Gi}	Generator's active power of i-th bus.
P_{is}	Active powers injection of TSCS unit into the i-th bus.
P_{ji}	Active power flows, respectively between i-th and j-th bus.
P_{Li}	The active power load of i-th bus.
p_i^k	personal bet postion of particle.
Q_{Gi}	Generator's reactive power of i-th bus.
Q_{is}	Reactive powers injection of TSCS unit into the i-th bus.
Q_{ji}	Active and reactive power flows, respectively between i-th and j-th bus.
Q_{Li}	The reactive power load of i-th bus.
Q_{ci}^{min}, Q_{ci}^{Max}	The i-th shunt capacitor's minimum and maximum VAR injection limits.
$r1, r2$	Random values.
R_{ij}	Transmission line resistance between the i-th and j-th buses.
S_{Li}, S_{Li}^{Max}	Apparent and maximum apparent power flow limit of the i-th branch. N: The number of transmission lines
T_i^{min}, T_i^{Max}	The $i-th$ transformer's minimum and maximum tap setting limits.
V_i, V_j	Voltage magnitudes at i-th and j-th bus respectively.
V_{Li}^{min}, V_{Li}^{Max}	lower and upper load voltages of i-th load bus.
v_i^k	Velocity vector of particle.
W_i	Weight factor.
X_{ij}	Transmission line reactance between the i-th and j-th buses.
X_{TCSCij}	The TSCS's reactance in the transmission line that connects the i-th and j-th buses.
X_{TCSCi}^{min}, X_{TCSCi}^{Max}	The maximum and minimum limits of the of the i-th TCSC reactance.
Y_{ih}	The transmission line admittance between the i-th and j-th bus.
z_1	Array of dependent variables.
z_2	Array of independent variables.
$\boldsymbol{z_i^k}$	Particles' vector position.
$z_{B,j}^k$, $z_{c,j}^k$, Z_{best}^k	Prey's position, Cheetah's current position, and cheetah's best position
δ_i, δ_j	Angles at i-th and j-th bus respectively.

References

[1] M. Al-Kaabi, V. Dumbrava, and M. Eremia. "Single and Multi-Objective Optimal Power Flow Based on Hunger Games Search with Pareto Concept Optimization", *Energies*, Vol. 15, No. 22, pp. 1-33, 2022, doi: 10.3390/en15228328

[2] U. Guvenc, B. E. Altun, and S. Duman, "Optimal power flow using genetic algorithm based on similarity", *Energy Education Science and Technology Part A: Energy Science and Research*, Vol. 29, No.1, pp. 1-10, 2012.

[3] J. Carpentier, "Contribution a l'etude du dispacting economique", Bull. Soc. Francaise des Electriciens, Vol. 3, pp. 431−447, 1962.

[4] D. I. Sun, B. Ashley, B. Brewer, A. Hughes, W.F. Tinney, Optimal power flow by Newton approach, IEEE Transaction on Power Apparatus and Systems, Vol. PAS-103, No. 10, pp. 2864-2880, 1984.

[5] A. Ramos, I. J. Perez-Arriaga, J. Bogas, "A nonlinear programming approach to optimal static generation expansion planning", *IEEE Transactions on Power Systems*, Vol. 4, No.3, pp. 1140-1146, 1989.

[6] J. Lavei, A. Rantzer, and S. Low, "Power flow optimization using positive quadratic programming", IFAC Proceedings Volumes. Vol. 44, No.1, pp. 10481-10486, 2011.

[7] J. P. Dedieu, and M. Shub, "Newton flow and interior point methods in linear programming", *International Journal* of *Bifurcation* and *Chaos*, Vol.15, No.3, pp. 827-839, 2005.

[8] A. Castillo and R. P. Oneill, "Survey of Approaches to Solving the ACOPF", *Tech. Rep., 2013.*

[9] B. Mallala, D. Dwivedi, "Salp swarm algorithm for solving optimal power flow problem with thyristor-controlled series capacitor", *Journal of Electronic Science and Technology*, Vol.20, No.2, pp.1-9, 2022.

[10] J. C. Bansal, S. S. Jadon, R. Tiwari, D. Kiran and B. K. Panigrahi. "Optimal power flow using artificial bee colony algorithm with global and local neighbourhoods", *International Journal of System Assurance Engineering and Management*, Vol. 8, pp. 2158-2169, 2014.

[11] M. A. Abido, "Optimal power flow using particle swarm optimization", *International Journal of Electrical Power & Energy Systems*, Vol. 24, No.7, pp. 563-571, 2002.

[12] J. A, Regalado, E. E. Barocio and E. Cuevas. "Optimal power flow solution using Modified Flower Pollination Algorithm", *IEEE*

International Autumn Meeting on Power, Electronics and Computing (ROPEC), Ixtapa, Mexico*,* pp. 1-6, 2015.

[13] L. H Abood, R. Haitham, "Design an optimal fractional order PI controller for congestion avoidance in internet routers. Mathematical Modelling of Engineering Problems", Vol.55, No.6, PP.1321-1326, 2022.

[14] A. M. Abed, A. A. Alkhazraji, and Sh. S. A. Al-Kubragyi "Modelling and Simulation of an on Grid 100-kw Photovoltaic system", *International Journal of Power Electronics and Drive System (IJPEDS)*, Vol.14, No.3, pp.1651-1659, 2023.

[15] A. F. Shafeeq, and I. I. Ali, "Proper insertion of DSTATCOM in distribution networks based on VSM with network reconfiguration", *Indonesian Journal of Electrical Engineering and Computer Science*, Vol.29, No. 1, PP. 66-74, 2023.

[16] A. Mukherjee, and V. Mukherjee, "Solution of optimal power flow with FACTS devices using a novel oppositional krill herd algorithm", *International Journal of Electrical Power & Energy Systems*, Vol. 78, pp. 700-714, 2016.

[17] A. F. Shafeeq, and I. I. Ali, "Simple Strategy for Finding Optimal Location and Size of Distributed Generators and SVC Devices in Radial Distribution Systems", *International Journal of Intelligent Engineering and Systems* , Vol. 15, No.5, PP. 261-272, 2022.

[18] A. Tiwari and K. K. Swarnkar, "Optimal Power Flow with Facts Devices using Genetic Algorithm", *International Journal of Power System Operation and Energy Management*, Vol. 1, No.3, 2012.

[19] D. Prasad, and V. Mukherjee. "A novel symbiotic organisms search algorithm for optimal power flow of power system with FACTS devices", *Engineering Science and Technology, an International Journal*, Vol. 19, No.1, pp. 79-89, 2016.

[20] N. H. Khan, Y. Wang, D. Tian, R. Jamal, S. Iqbal, M. Abdulrahman A. S., and M. Ebeed "A Novel Modified Lightning Attachment Procedure Optimization Technique for Optimal Allocation of the FACTS Devices in Power Systems", *in IEEE Access*, Vol. 9, pp. 47976-47997, 2021.

[21] W. Yi, Z. Lin, Y. Lin, S. Xiong, Z. Yu and Y. Chen, "Solving Optimal Power Flow Problem via Improved Constrained Adaptive Differential Evolution", *Mathematics*, MDPI, Vol. 11, No.5, pp.1-13, 2023.

[22] H. Alnami, A. M. El-Rifaie, G. Moustafa, S. H. Hakmi, A. M. Shaheen and M. A. Tolba, "Optimal Allocation of TCSC Devices in Transmission Power Systems by a Novel Adaptive Dwarf Mongoose Optimization", *in IEEE Access*, Vol. 12, pp. 6063-6087, 2024.

[23] M. Balasubbareddy, D. Dwivedi, and P.V. Prased, "Optimal power flow solution using HFSS Algorithm", *Journal of Electrical and Electronics Engineering Research*, Vol. 12, No. 1, pp. 1-11, 2023.

[24] L. Shimin, H. Chen, M. Wang, A. Asghar Heidari, and S. Mirjalili. "Slime mould algorithm: A new method for stochastic optimization", *Future Generation Computer Systems 111*, pp. 300-323, 2020.

[25] M. A, Akbari, M. Zare, R. Azizipanah-Abarghooee, S. Mirjalili, M. Deriche, "The Cheetah Optimizer: A Nature-Inspired Metaheuristic Algorithm for Large-Scale Optimization Problems", *Scientific Report*, Vol. 12, p. 10953, 2022, doi: 10.1038/s41598-022-14338-z

[26] H. Abdelhadi, A. M. Mahmoud, E. M. Saied, M. A. Mohamed, "Innovative hierarchical control of multiple microgrids: Cheetah meets PSO", *Energy Reports*, Vol. 11, pp. 4967-4981, 2024.

[27] Z A. Memon, M. A. Akbari, M. Zare, "An Improved Cheetah Optimizer for Accurate and Reliable Estimation of Unknown Parameters in Photovoltaic Cell and Module Models", *Applied Sciences*, Vol. 13, No. 18, pp. 1-31, 2023.

[28] A. Pratap, P. Tiwari, R. Maurya, B. Singh, "Cheetah Optimization Algorithm for Simultaneous Optimal Network Reconfiguration and Allocation of DG and DSTATCOM with Electric Vehicle Charging Station", *Serbian Journal of Electrical Engineering*, Vol. 21, No. 1, pp. 1-37, 2024.

[29] S. Wafaa, and L. Tawfeeq. "Voltage Collapse Optimization for the Iraqi Extra High Voltage 400 kV Grid based on Particle Swarm Optimization", *Iraqi Journal for Electrical & Electronic Engineering*, Vol. 13, No. 1, 2017.